Filter gate closure inhibits ion but not water transport through potassium channels

Torben Hoomann[a], Nadin Jahnke[b], Andreas Horner[a], Sandro Keller[b], and Peter Pohl[a,1]

[a]Institute of Biophysics, Johannes Kepler University of Linz, 4020 Linz, Austria; and [b]Molecular Biophysics, University of Kaiserslautern, 67663 Kaiserslautern, Germany

Edited by Ramon Latorre, Centro Interdisciplinario de Neurociencias, Universidad de Valparaíso, Valparaíso, Chile, and approved May 23, 2013 (received for review March 11, 2013)

The selectivity filter of K^+ channels is conserved throughout all kingdoms of life. Carbonyl groups of highly conserved amino acids point toward the lumen to act as surrogates for the water molecules of K^+ hydration. Ion conductivity is abrogated if some of these carbonyl groups flip out of the lumen, which happens (*i*) in the process of C-type inactivation or (*ii*) during filter collapse in the absence of K^+. Here, we show that K^+ channels remain permeable to water, even after entering such an electrically silent conformation. We reconstituted fluorescently labeled and constitutively open mutants of the bacterial K^+ channel KcsA into lipid vesicles that were either C-type inactivating or noninactivating. Fluorescence correlation spectroscopy allowed us to count both the number of proteoliposomes and the number of protein-containing micelles after solubilization, providing the number of reconstituted channels per proteoliposome. Quantification of the per-channel increment in proteoliposome water permeability with the aid of stopped-flow experiments yielded a unitary water permeability p_f of $(6.9 \pm 0.6) \times 10^{-13}$ cm^3·s^{-1} for both mutants. "Collapse" of the selectivity filter upon K^+ removal did not alter p_f and was fully reversible, as demonstrated by current measurements through planar bilayers in a K^+-containing medium to which K^+-free proteoliposomes were fused. Water flow through KcsA is halved by 200 mM K^+ in the aqueous solution, which indicates an effective K^+ dissociation constant in that range for a singly occupied channel. This questions the widely accepted hypothesis that multiple K^+ ions in the selectivity filter act to mutually destabilize binding.

membrane channels | protein reconstitution | knock-on mechanism | aquaporin | brain water homeostasis

Impulse propagation in the central nervous system and in other excitable tissues is unthinkable without ion-selective channels. Membrane depolarization and repolarization in the course of an action potential require Na^+ to be excluded from K^+ channels, and vice versa (1). Although eukaryotic ion-channel researchers have tried for decades to figure out how nature accomplishes such a size-independent selectivity mechanism, it has long remained enigmatic (2). The problem then was solved by the structure of the prokaryotic K^+ channel KcsA (3), even though its host organism, *Streptomyces lividans*, lacks excitability. Hence, crucial developments in deciphering the selectivity mechanism have emerged owing to KcsA's lack of a voltage sensor domain and auxiliary subunits (e.g., ref. 4) as a result of the reduced complexity of KcsA compared with human K^+ channels.

In all K^+ channels, the selectivity filter is made up of a conserved sequence of amino acids with their carbonyl groups pointing toward the lumen of the channel to act as surrogates for the waters of K^+ hydration (5). Gradual reorientation of the filter backbone leads to a loss of these surrogates at two of the four ion-binding sites in the filter, which in turn abrogates ion conduction (6). This process is called C-type inactivation and, just like the selectivity mechanism, is preserved in the eukaryotic kingdom of life (e.g., ref. 7). The lack of a physical pore block suggests that (*i*) the C-type inactivated channel pore might remain permeable to water and (*ii*) maintenance of osmotic equilibrium is the physiological function of the C-type inactivated state. This hypothesis is supported by the observation that KcsA provides an extremely efficient water pathway. The reported single-channel water permeability $p_f = 4.8 \times 10^{-12}$ cm^3·s^{-1} (8) exceeds that of channels specialized in water transport by more than an order of magnitude (9). For example, the p_f values for aquaporin-1 and aquaporin-4 amount to 0.6–1.1 and 2.4×10^{-13} cm^3·s^{-1}, respectively (10, 11).

The goal of the present paper is to clarify whether C-type inactivated K^+ channels may act as water channels. To answer this question, we use the model channel KcsA and exploit the fact that the structures of the inactivated (12) and collapsed (6) filters are virtually indistinguishable (Fig. 1). The main difference is that the C-type inactivated state may occur in the presence of 150 mM K^+ in the cytoplasm, whereas the collapsed state requires a reduction in K^+ concentration to a few millimolars on both sides of the membrane (5). We tested whether the inactivated/collapsed channel and the noninactivating mutant E71A (13) have the same p_f. In both channels, we kept the cytoplasmic gate constitutively open by introducing the mutations H25R and E118A, which render the channels insensitive to pH (14). Reconstitution of the purified channels into lipid vesicles and determination of channel abundance by fluorescence correlation spectroscopy (FCS) (15) allowed the observation of water flow through the inactivated/collapsed state.

Results

We overexpressed and purified pH-insensitive (*i*) noninactivating (H25R/E71A/E118A) and (*ii*) inactivating (H25R/E118A) mutants of the KcsA channel. Unwanted spontaneous fusion of proteoliposomes at low pH was avoided by using pH-insensitive mutants (14). In addition, serine at position 6 was substituted for cysteine, enabling the attachment of the fluorescent dye ATTO 488. Protein reconstitution by exchanging detergent for *Escherichia coli* polar lipid extract supplemented with 0.01% *N*-(lissamine rhodamine B sulfonyl) phosphatidylethanolamine resulted in proteoliposomes in which the protein and some lipids were labeled with distinct fluorescent dyes.

We subjected a small fraction of the vesicle suspension to FCS to determine the number of KcsA channels per vesicle (Fig. 2). We first measured the number of vesicles in the confocal volume. The higher particle count w_L in the lipid channel compared with that in the protein channel w_P was partly a result of the larger confocal volume V_L of the lipid channel and partly a result of the

Author contributions: P.P. designed research; T.H., N.J., and A.H. performed research; N.J., A.H., and S.K. contributed new reagents/analytic tools; T.H. and P.P. analyzed data; and S.K. and P.P. wrote the paper.

The authors declare no conflict of interest.

This article is a PNAS Direct Submission.

Freely available online through the PNAS open access option.

[1]To whom correspondence should be addressed. E-mail: peter.pohl@jku.at.

This article contains supporting information online at www.pnas.org/lookup/suppl/doi:10.1073/pnas.1304714110/-/DCSupplemental.

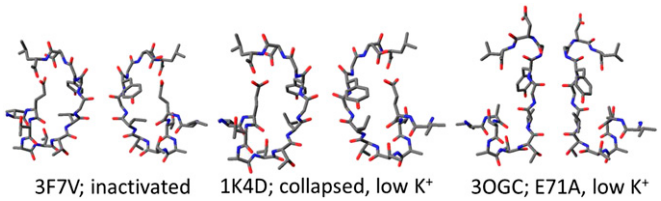

Fig. 1. Comparison of the inactivated (PDB ID code 3F7V, ref. 6), collapsed (low-K^+; PDB ID code 1K4D, ref. 5), and noninactivating (E71A; PDB code 3OGC, ref. 24) crystal structures of KcsA. In its open noninactivated state, KcsA is known to conduct both water and ions. In its collapsed or inactivated state, the channel is closed to ions. Assuming a low binding affinity of K^+ for these two states (31), we tested the hypothesis that, with an open cytoplasmic gate, both the inactivated and the collapsed states are permeable to water.

presence of a fraction of protein-free vesicles. In a second step, we dissolved the vesicles by adding detergent and determined the number w_M of particles in the protein channel again. Assuming that each labeled micelle detected in the protein channel contained exactly one KcsA tetramer, we calculated the average number n of KcsA channels per vesicle as $w_M V_L / w_L V_P$, where V_P is the confocal volume of the protein channel. Depending on the preparation, n varied between 0.7 and 3. Analogously, the average number m of KcsA channels per proteoliposome was taken as w_M/w_P.

All the reconstituted proteins were functional, as was revealed by fusion of the proteoliposomes with preformed planar bilayers (Fig. 3). These bilayers were folded from monolayers of *E. coli* polar lipid in an aperture of a diaphragm separating two aqueous compartments. Only one of the compartments contained proteoliposomes and salt at an elevated concentration. Each fusion event was indicated by an initial jump of the transmembrane current. When the H25R/E118A mutant was present, the current decreased in steps, each of which indicated the inactivation of one or several channels. By contrast, the current stayed nearly constant after the fusion of vesicles containing the reconstituted H25R/E71A/E118A mutant. The initial current amplitude allowed us to derive the number of KcsA channels per vesicle, which we found to be in very good agreement with m determined by FCS. For example, for the H25R/E118A mutant, we measured (2.5 ± 0.8) channels (mean ± SE) in five fusion experiments (Fig. 3*A*), whereas the corresponding m was equal to 2.5 ± 0.5. The respective numbers for the H25R/E71A/E118A mutant were equal to 2.9 ± 0.6 (Fig. 3*B*) and 2.6 ± 0.5, respectively.

Removal of the externally applied transmembrane potential facilitated the return of the inactivated filter to its conducting state. That is, when we reapplied the external potential after an interval of about 12 s, the previously inactivated channels reopened, and the current returned to its postfusion level (Fig. 3 *B* and *D*). This agrees well with the time dependence of the recovery from C-type inactivation observed for other K^+ channels (16).

Both the inactivating and the noninactivating mutants acted to increase the water permeability of proteoliposomes P_f beyond that of pure lipid vesicles $P_{f,l} = (29 \pm 3)$ μm·s^{-1}. The incremental permeability $P_{f,c}$ introduced by KcsA channels was measured in the presence of 9 mM K^+ inside the vesicles and in the external buffer. The volume V of the vesicles decreased upon exposure to an osmotic gradient of $c_{osm} = 0.3$ M sucrose in a stopped-flow apparatus, resulting in an increase in the intensity I of monochromatic light (wavelength 546 nm) scattered at an angle of 90°. We added both the K^+ carrier valinomycin and the protonophore carbonyl cyanide *m*-chlorophenyl hydrazone (CCCP) to the aqueous solution to prevent buildup of a membrane potential due to ions dragged by water through the channel, which would eventually stop transport. Once the membrane potential was thus clamped at zero, recordings of I as a function of time (Fig. 4) allowed calculation of the total osmotic permeability P_f of the vesicles as (17):

$$P_f = P_{f,c} + P_{f,l} = \frac{d}{6 V_W \tau_{SF} c_{osm}}, \quad [1]$$

where $d = 120$ nm, V_W, and τ_{SF} are the initial vesicle diameter, the molar volume of water, and the time constant of the single-exponential change in I, respectively. Because the vesicles shrank exponentially to ~60% of their initial volume, they retained ~75% of their volume at time point τ_{SF}. This is equivalent to a 9% change in diameter or to a change in the volume-to-surface ratio (d/6) of less than 2%. Eq. 1 assumes these changes are negligible.

Repeating the stopped-flow experiments for different values of n revealed that $P_{f,c}$ is proportional to n:

$$P_{f,c} = \frac{n p_f}{\pi d^2}, \quad [2]$$

allowing calculation of the unitary KcsA water permeability p_f from the slope of Fig. 5*A*:

$$\frac{1}{\tau_{SF}} = \frac{6 P_{f,l} c_{osm} V_W}{d} + \frac{6 c_{osm} V_W p_f}{\pi d^3} n, \quad [3]$$

to be equal to (4.1 ± 0.4) × 10^{-13} $cm^3 \cdot s^{-1}$ for both the H25R/E118A and the H25R/E71A/E118A mutants at 7 °C.

p_f indicates the mobility of water molecules (with radius r) inside the channel and thus is directly proportional to their diffusion coefficient D_W (18). This allows the use of p_f measurements for estimating D_W (19). Conversely, the Stokes–Einstein relation $D_W = kT/6\pi\eta r$ may be used to estimate p_f at room

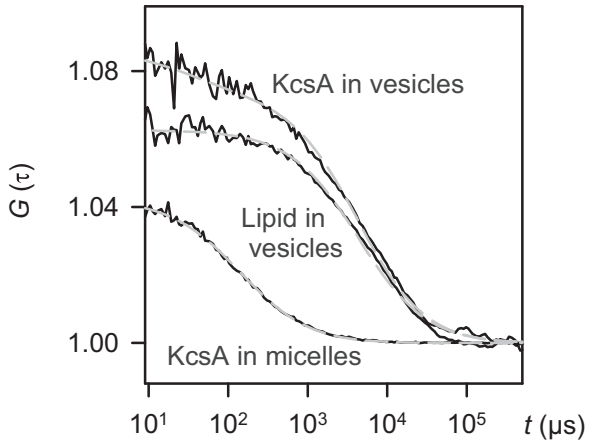

Fig. 2. FCS for counting the number of KcsA channels per vesicle. Autocorrelation curves obtained for the proteoliposome suspension were used to extract both the residence times τ_D and the numbers w_P and w_L of fluorescently labeled protein and lipid particles in the confocal volumes of green (488-nm) and red (633-nm) lasers, respectively, by fitting the standard model (dotted gray lines) for two-component free 3D diffusion (47) to $G(\tau)$. The residence time of the free dye was fixed at 25 μs. The difference in particle numbers between the KcsA and lipid channels was a result of different confocal volumes as well as the presence of both protein-containing and empty vesicles. Vesicle dissolution by OG at a final detergent concentration of 2% resulted in a decrease in τ_D from ~4.3 ms to ~200 μs. Assuming that each micelle contained one KcsA tetramer at most, we determined the number w_M of micelles in the confocal volume. After correction for dilution, the ratio $w_M V_L / w_L V_P = 2.84$ gives the number n of tetramers per vesicle and the ratio $w_M/w_P = 2.91$ the number m of tetramers per proteoliposome. V_L and V_P are the confocal volumes of the lipid and the proton channels, respectively. The buffer contained 150 mM KCl, 25 mM Tris, and 25 mM Hepes (pH 7.50).

PHYSIOLOGY

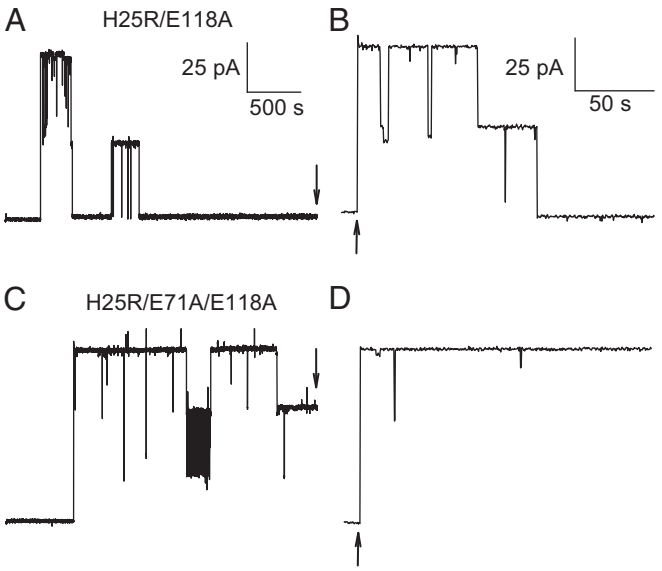

Fig. 3. Fusion of a single proteoliposome to a preformed planar bilayer. Ten microliters of a vesicle suspension (5 mg/mL) with the inactivating protein (*A* and *B*) or noninactivating mutant (*C* and *D*) was added to the hyperosmotic compartment (260 mM KCl). The hypoosmotic compartment contained 150 mM KCl. Solutions were buffered with 25 mM Tris and 25 mM Hepes (pH 7.50). Vesicle fusion resulted in the insertion of KcsA channels into the bilayer, as indicated by a sudden increase in current (*A* and *C*). Subsequently, the current decreased in a stepwise manner upon channel inactivation. The constant voltage of +100 mV was turned off (↓) and switched on again after a total of about 12 s (↑). At that time, all channels had recovered from inactivation, as indicated by the current amplitude. Note the 10-fold expanded time scale in *B* and *D* compared with *A* and *C*.

temperature. In doing so, we exploit that the viscosity, η, of water is close to its bulk value even when confined in monomolecular films (20, 21). Because η decreases from 1.5 centipoise (cP) at 7 °C to 0.89 cP at 25 °C (22), we estimate p_f to be equal to $(6.9 \pm 0.6) \times 10^{-13}$ cm^3·s^{-1} at 25 °C (Fig. 5*B*).

For some K^+ channels, total removal of K^+ from the medium may lead to an irreversible loss of K^+ conductance (23). Therefore, we subjected K^+-free proteoliposomes to the same fusion procedure as the above-mentioned K^+-containing proteoliposomes to test whether this also was the case for KcsA. We obtained current traces (Fig. S1) with indistinguishable single-current characteristics, suggesting that (*i*) channel stability does not require K^+ and (*ii*) entering the collapsed state is fully reversible. Subsequently, we used the K^+-free proteoliposomes to again determine p_f for the "collapsed" H25R/E118A and the H25R/E71A/E118A mutants, this time in K^+-containing buffer. The p_f values did not differ significantly from those obtained in the presence of 9 mM K^+ (Fig. 5).

K^+ concentrations of 300–400 mM are required for complete blockage of water flux through the KcsA pore (8). We added 200 mM K^+ to the remainder of the proteoliposome population (Fig. 4) after measuring $P_{f,c}$ at low K^+. In the presence of valinomycin and CCCP, internal and external K^+ concentrations rapidly equilibrated. Subsequent exposure to $c_{osm} = 0.3$ M sucrose in the stopped-flow apparatus revealed an invariant $P_{f,i}$ but a decrease in $P_{f,c}$, from which we calculated a p_f of about $(2.5 \pm 0.3) \times 10^{-13}$ cm^3·s^{-1}. This reduction in p_f is in qualitative agreement with single-file movement of K^+ and water.

Discussion

Both channel inactivation [Protein Data Bank (PDB) ID code 3F7V] and collapse of the selectivity filter at very low K^+ concentration (PDB ID code 1K4D) are thought to close K^+ channels (5). In other words, the filter is believed to act as a second gate in K^+ channels. Here, we show that the closure of this second gate is incomplete: while inhibiting the passage of ions, the "closed" gate still permits the passage of water molecules. In this regard, it differs from the first gate at the cytoplasmic entrance, which opens and closes K^+ channels to both ions (5) and water molecules (8).

In the absence of K^+, the H25R/E118A mutant must have entered a state that is structurally indistinguishable from the C-type inactivated state (6). Nevertheless, p_f of this collapsed state was similar to the one of the H25R/E71A/E118A mutant (Fig. 5), which does not inactivate, even in the absence of K^+ (24). We conclude that filter inactivation/collapse is unlikely to alter the rate-limiting step of water permeation through KcsA.

According to

$$D_W = \frac{3Np_f}{\pi r_p} \quad [4]$$

(18, 19), a p_f of $(6.9 \pm 0.6) \times 10^{-13}$ cm^3·s^{-1} corresponds to a diffusion coefficient D_W of water molecules inside the channel of $\sim 1.8 \times 10^{-4}$ cm^2·s^{-1}, which exceeds D_W of bulk water. r_p and N denote the pore radius and the number of water molecules in

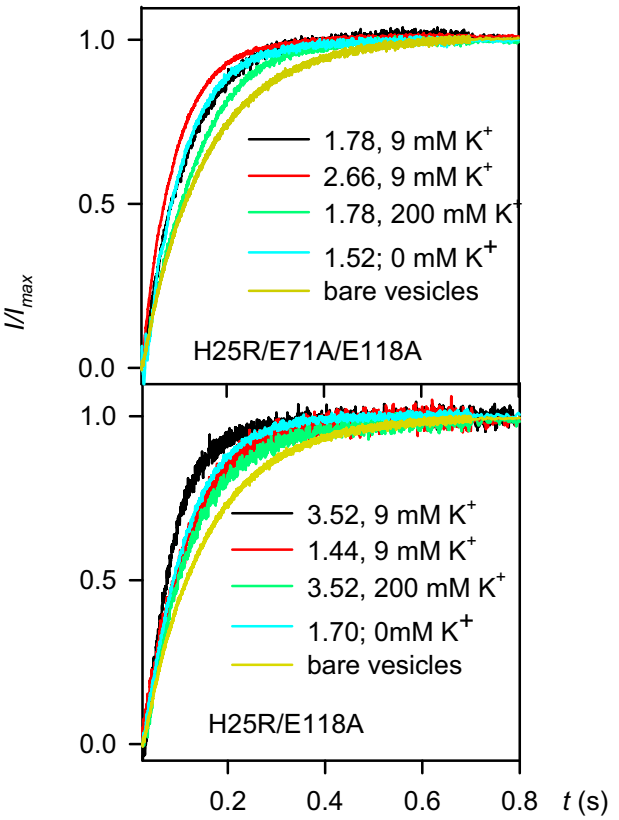

Fig. 4. Osmotic water permeability of proteoliposomes. Stopped-flow experiments were performed in the presence of 8 μM valinomycin and 5 μM CCCP. Two populations of vesicles were used: with 0 (cyan lines) and 9 mM K^+ (black and red lines) on both the inside and outside. The average number of KcsA tetramers per vesicle is indicated. Dilution (1:1 vol/vol) of the vesicle suspension in buffer (150 mM choline chloride, 25 mM Tris, 25 mM Hepes, pH 7.50) containing 600 mM sucrose resulted in vesicle shrinkage. Partial inhibition of KcsA-mediated water flow was achieved by increasing the K^+ concentration to 200 mM (green lines). To this end, the 9 mM K^+ vesicle population (black lines) first was incubated in 200 mM K^+ buffer and then subjected to a stopped-flow experiment. Measurements were done at 7 °C. Experimental traces were fitted by a single-exponential function to determine the characteristic time τ_{SF}.

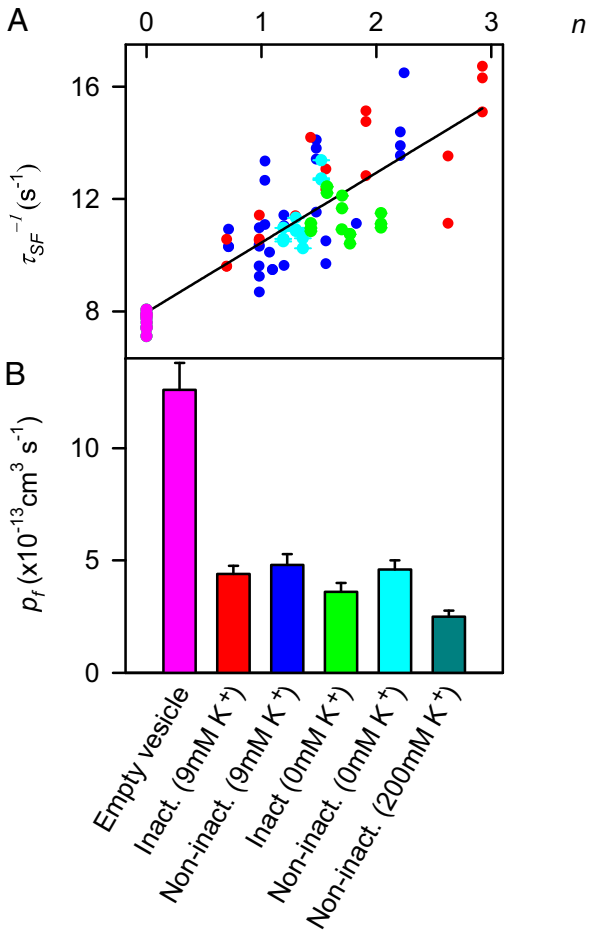

Fig. 5. Single-channel water permeability. (*A*) τ_{SF}^{-1} is plotted as a function of *n*. τ_{SF}^{-1} and *n* were determined in experiments such as those shown in Figs. 4 and 2, respectively. The color of the data points corresponds to the color of the bars in *B*. Using Eqs. 2 and **3**, a linear fit (black line) through all data points allowed calculation of $p_f \sim (4.1 \pm 0.4) \times 10^{-13}$ cm^3·s^{-1}. (*B*) Individual p_f values (with SE) calculated similarly for the inactivating mutant (Inact.; H25R/E118A) and the noninactivating mutant (Non-inact.; H25R/E71A/E118A) at 0, 9, and 200 mM KCl in both the vesicle interior and the buffer solutions. p_f of an empty lipid vesicle was defined as the water permeability of a lipid bilayer $P_{f,l}$ multiplied by the surface area of one vesicle. The decrease in K^+ concentration from 9 to 0 mM had no significant effect on water flow, whereas the increase in K^+ concentration from 9 to 200 mM led to partial inhibition.

the pore, respectively. Because transport through the narrow selectivity filter is the rate-limiting step and because the filter must be empty of ions to allow fast water movement (see the calculation of turnover numbers below), *N* must be equal to 4 (8). Thus, water is rushing through the filter unhindered by interactions with the channel wall. The increase in D_W compared with bulk water mobility may be a result of the reduced number of hydrogen bonds within the channel. Single-file water molecules with comparably high mobility also have been observed inside other membrane pores (19, 25).

Previously, D_W was calculated at $\sim 1.2 \times 10^{-3}$ cm^2·s^{-1} for single-file water molecules inside wild-type KcsA (19). The number of open channels *n* was determined as the ratio *G*/*g*, where *G* and *g* denote the steady-state integral conductance of the whole lipid bilayer and the single-channel conductance of KcsA, respectively (8). Ninety percent of all channels were likely to inactivate during the measurement of *G* (13). These inactivated channels, which according to our present results are closed only for ions but open to water, were neglected. Thus, *n* of the water-conducting channels was underestimated by 10-fold. If we account for all water-conducting channels, p_f and D_W of the previous study (8) are reduced to 4.8×10^{-13} cm^3·s^{-1} and 1.2×10^{-4} cm^2·s^{-1}, respectively. These values are in reasonable agreement with the respective values 6.9×10^{-13} cm^3·s^{-1} and 1.8×10^{-4} cm^2·s^{-1} of the current study, particularly if the methodical differences between scanning electrochemical microscopy (8) and stopped flow are taken into account. The above considerations imply that the channel does not collapse or inactivate during water-flow measurements. Bulk K^+ concentrations ≥9 mM are compatible with this view. Although osmotic water flow through the filter sweeps away ions, the experimental conditions ensure multiple visits of K^+ to all binding sites within the time required for inactivation (26). Thus, there is only a small probability of filter collapse, as documented by X-ray crystallography for a lone K^+ equilibrated in its binding pocket (5, 27). Clamping the transmembrane voltage at zero additionally diminishes the probability of entering the inactivated state (compare Fig. 3 and ref. 28).

Knowledge of p_f allows calculation of the water turnover number of KcsA (29) as $M_w = N_A p_f / V_w = 2.3 \times 10^{10}$ molecules per second, where N_A is Avogadro's number. The highest turnover number M_K reported for K^+ is $\sim 1.8 \times 10^8$ ions per second (12). The 100-fold difference suggests that the presence of K^+ in the selectivity filter inhibits fast water flow (8). However, experimentally, the water permeability of the noninactivating mutant in the presence of 200 mM K^+ is still about 60% of the maximum value (Fig. 5), which raises the question as to whether the single-file transport mechanism still applies.

There are three alternative explanations: The first is that water does not flow through the ion channel per se but at the protein–lipid interface, because the channel might perturb the lipid membrane. However, the complete inhibition of water flow previously observed when Na^+ blocks the pore (8) renders this explanation rather unlikely. The second possibility is that water flows through an alternative pathway within KcsA at a high rate. According to molecular dynamics simulations, this water route localizes behind the selectivity filter and provides a p_f of $(2.3 \pm 0.7) \times 10^{-13}$ cm^3·s^{-1} (30). However, this scenario necessitates that the channel be in its collapsed (i.e., low-K^+) state (30). Although our noninactivating mutant never enters the collapsed state (24), it still conducts water at the same rate as the other channels (Figs. 4 and 5), which renders the *in silico* model implausible. The third possibility involves water traversing the selectivity filter, which has widened to an extent that water and K^+ ions may pass each other. If this were the case, the partially hydrated Na^+ also would permeate. We can rule out this scenario because (*i*) Na^+ blocks the pore (8), and (*ii*) KcsA is stable in the absence of K^+ in vitro (Fig. S1) and (*iii*) also *in silico* (31).

The exclusion of alternatives suggests that fast water transport through KcsA occurs in a single-file fashion through the central pore. $M_w >> M_K$ indicates a much smaller p_f of the channel that contains either one or two ions vs. that of the cation-free channel. Consequently, the water permeability of the channels at activity *a* relative to that in the absence of cations $P_{f,c}(a)/P_{f,c}(0)$ is (32)

$$\frac{P_{f,c}(a)}{P_{f,c}(0)} = \left(1 + \frac{a}{K_1} + \frac{a^2}{K_1 K_2} + \dots\right)^{-1}, \qquad [5]$$

where K_1 and K_2 are the dissociation constants for the first and second cation, respectively. Unfortunately, K_1 and K_2 are not known. Eq. 5 may be simplified because most of the channels do not contain an ion, as follows from $P_{f,c}(a)/P_{f,c}(0) \sim 0.6$ (Fig. 5) of the noninactivating mutant at 200 mM K^+. Consequently, the fraction of channels with double occupancy is rather small, which renders the quadratic and all higher terms in Eq. 5 negligible. If the association constant k_{on} is that of a diffusion-limited process

(i.e., $\sim 10^8\ M^{-1}\cdot s^{-1}$) and the off-rate is roughly equal to M_K, $K_1 = M_K/k_{on}$ must be in the order of 1 M (27). Nelson (33) calculated an effective dissociation constant of 310 mM and a k_{on} value of $\sim 2.2 \times 10^8\ M^{-1}\cdot s^{-1}$ from the current voltage curves of a MaxiK channel. Taking his dissociation constant for K_1, we calculate $P_{f,c}(a)/P_{f,c}(0) = 0.6$ from Eq. 5. This theoretical prediction is in very good agreement with our experimental result, lending credence to a single-file transport mechanism.

Much smaller equilibrium dissociation constants of 2–7 μM, 29 μM, or 430 μM have been found by NMR (26), measurements of Ba^{2+} block as a function of extracellular K^+ concentration (34), and isothermal titration calorimetry (ITC) when Li^+ inside the filter was substituted for K^+ (27), respectively. According to current models of K^+ transport (35, 36), these constants are replaced by those larger by three or four orders of magnitude only when a second ion enters the filter and electrostatically destabilizes the first ion. However, this knock-on mechanism (36) cannot explain our observation of K_1 on the order of 300 mM for a singly occupied KcsA channel. Furthermore, it does not agree well with the micromolar dissociation constant of K^+ in coresidency with divalent Ba^{2+}. If an electrostatic destabilization mechanism had been at work here, this constant should have been much larger than the one affected by coresidency with a second K^+ (34).

The pronounced dependence of ion affinity on the distance to the coordinating carbonyl oxygens may provide an alternative explanation. That is, it would be sufficient if the oxygen positions of the water-conducting conformation in our experiments differed by less than 1 Å from those steady-state positions probed by NMR, ITC, or Ba^{2+} block to attain an increase in the effective dissociation constants by three or four orders of magnitude. For example, the radius of Na^+ is only 0.42 Å smaller than that of K^+, but the binding affinity of the former is so low that it cannot replace Li^+ in ITC experiments (27) or suppress Ba^{2+} escape from the filter (34).

Another consequence of its smaller radius is that Na^+ does not enter the cage cornered by eight carbonyl oxygens (as does K^+) but instead binds in the plane of only four carbonyl oxygens (37, 38). Those of T75 provide a site of particularly high affinity for both Na^+ and Li^+ according to both crystal structures [PDB ID codes 2ITC (27) and 3GB7 (37), respectively] and molecular dynamics simulations (37). For Na^+ to reach this site, the filter must be empty of K^+ (37). This requirement is met during osmotic water flow, which explains the capability of Na^+ to block it (8). Na^+ does not block the K^+ current because the 1-Å shift of its binding site closer to the K^+ binding site creates an energy barrier that Na^+ has to overcome to enter a K^+-containing selectivity filter (38).

At the moment, the physiological importance of water flux through C-type inactivated K^+ channels is unclear. However, it is known that eukaryotic K^+ channels also undergo C-type inactivation (39). These channels are expected to make a significant contribution to water flux only in places where they are highly abundant, because the lipid matrix offers a high background permeability. This is the case, for instance, in the synapses of the mammalian brain, where two C-type inactivating K^+ channels are found: Kv1.1, a major constituent of the presynaptic membrane, and Kir4.1, a channel in the plasma membrane of astrocytes of the perivascular end-feet. Water flow through these channels could make a physiologically meaningful contribution to the equilibration of the local osmotic gradient, which is generated by removal of K^+ from the synapse. This might be the case, for example, in astrocytic aquaporin-4 dysfunction, as this water channel currently is thought to be the sole facilitator of water flow out of the synapse (40). In addition, K^+ channels might be key in answering the question about the means for equilibrating the osmotic gradient generated by K^+ entry into the synapse.

Further efforts are required to elucidate the potential importance of C-type inactivated channels for brain water homeostasis. So far, all we know is that the C-type inactivated/collapsed prokaryotic K^+ channel KcsA conducts water at least as efficiently as aquaporins, and structural similarities to other C-type inactivating mammalian K^+ channels suggest that selective water transport through inactivated K^+ channels may be physiologically relevant.

Materials and Methods

Protein Expression and Purification. The mutants H25R/E118A and H25R/E71A/E118A were coded in the vector pASK75 (41). These plasmids were kindly provided by Crina Nimigean (Cornell University, New York City, NY). An S6C mutation was introduced into both plasmids using a QuikChange mutagenesis kit (Stratagene) and verified by sequencing the entire KcsA-coding sequence. For expression, we used *E. coli* strain BL21. Expression was induced by tetracycline, and the protein was purified after solubilization with 2% (wt/vol) octyl glucoside (OG) (42).

Protein Labeling. We followed a published protocol with only minor modifications (43). The KcsA–detergent solution was passed over an Ni^{2+}-chelating column. The eluate (elution buffer: 150 mM KCl, 2% OG, 3 mM KH_2PO_4, 300 mM imidazole, pH 7.80) was separated from imidazole by size-exclusion chromatography (Superdex 200; GE Healthcare), concentrated, and incubated with Tris(2-carboxyethyl)phosphine (Aldrich) for 5 min at 4 °C. ATTO 488 maleimide was added at 100 μM, and the solution was incubated overnight under constant mixing at 4 °C. The sample was diluted with buffer (150 mM KCl, 2% OG, 3 mM KH_2PO_4, pH 7.80) to reduce the imidazole concentration to <10 mM and mixed with Ni^{2+}-nitrilotriacetic acid beads for 30 min at 4 °C. After washing with 50 mL of the same buffer, the eluted protein again was subjected to size-exclusion chromatography and reconstituted as described below.

Protein Reconstitution into Small Unilamellar Vesicles. Sonicated unilamellar vesicles composed of *E. coli* polar lipid extract (Avanti Polar Lipids) at a lipid concentration of 28 mg/mL buffer (150 mM KCl, 25 mM Tris, 25 mM Hepes, pH 7.50) were added to the solubilized protein in small steps until reconstitution was complete (44, 45). This process was followed by buffer exchange via ultracentrifugation, resuspension of the vesicles, and a final dialysis step.

FCS. FCS served to measure the reconstitution efficiency (46). In brief, the average residence time τ_D and the number of proteoliposomes or micelles containing ATTO 488-labeled KcsA in the confocal volume were derived from the autocorrelation function $G(\tau)$ of the fluorescence temporal signal, which was acquired using a commercial laser scanning microscope equipped with avalanche diodes (LSM 510 META Confocor 3; Carl Zeiss). To this end, we applied the standard model for one-component free 3D diffusion (47). D was determined as $\omega^2/4\tau_D$. A water droplet formed the connection between the 40× water immersion objective and the coverslip, which provided the base of the measurement chamber.

KcsA Reconstitution into Planar Lipid Bilayers by Proteoliposome Fusion. Planar bilayers were formed from *E. coli* polar lipid extract dissolved in hexane. Lipid monolayers were formed by spreading the lipid solution on top of the aqueous phases on both *cis* and *trans* sides of a septum separating these phases (48). After evaporation of the solvent, the buffer solution (150 mM KCl, 25 mM Tris, 25 mM Hepes, pH 7.50) levels of both compartments were raised above the aperture (pretreated with a 0.5% solution of hexadecane in hexane) so that the two monolayers spontaneously combined to form a bilayer. Proteoliposomes were added to the *cis* compartment and fused with the preformed planar bilayer by increasing the KCl concentration to 260 mM.

Single Ion Channel Measurements. The transmembrane current was measured by a patch clamp amplifier (EPC9; HEKA) under voltage clamp conditions via Ag/AgCl reference electrodes. The recording filter was a four-pole Bessel with 3-dB corner frequency of 500 Hz. Raw data were analyzed using the TAC software package (Bruxton Corporation). Gaussian filters of 79 Hz were applied to reduce noise.

Stopped-Flow Measurements. Proteoliposomes or control vesicles were diluted 10-fold in buffer (150 mM choline chloride, 25 mM Tris, 25 mM Hepes,

pH 7.50) and extruded through two stacked 100-nm polycarbonate filters (Avestin). After 30 min of incubation with 8 μM valinomycin and 5 μM CCCP (both from Sigma), 75 μL of the suspension was mixed with the same volume of buffer containing 600 mM sucrose in a stopped-flow device (model SFM-300; Bio-Logic). Vesicle shrinkage was indicated by a change in the intensity of 546-nm light scattered at an angle of 90°. Measurements were done at +7 °C. Recording settings were 7,000 data points at an interval of 100 μs and 1,000 data points at an interval of 2 ms with a filter of 300 μs according to the manufacturer's recommendations. Within 2.6 s, the curves saturated to the final scattering intensity. An average of 8–12 curves were obtained for each time trace used for analysis. The curves were offset-corrected, normalized to I/I_{max}, and fitted by a single-exponential function.

ACKNOWLEDGMENTS. We thank Crina Nimigean (Cornell University) for providing plasmids of pH-insensitive KcsA mutants and Francisco Bezanilla (University of Chicago) for introducing us to the protein labeling technique and for critically reading the manuscript. We are indebted to Ramon Latorre (Universidad de Valparaíso) for helpful comments on the manuscript and to Quentina Beatty (Johannes Kepler University) for editorial help. This project was supported by Grant P19716 from the Austrian Science Fund (Fonds zur Förderung der Wissenschaftlichen Forschung; to P.P.) and Grant 961-386261/969 from the Stiftung Rheinland-Pfalz für Innovation (to S.K.).

1. Bezanilla F (2006) The action potential: From voltage-gated conductances to molecular structures. *Biol Res* 39(3):425–435.
2. Miller C (2001) See potassium run. *Nature* 414(6859):23–24.
3. Doyle DA, et al. (1998) The structure of the potassium channel: Molecular basis of K^+ conduction and selectivity. *Science* 280(5360):69–77.
4. Contreras GF, Neely A, Alvarez O, Gonzalez C, Latorre R (2012) Modulation of BK channel voltage gating by different auxiliary β subunits. *Proc Natl Acad Sci USA* 109(46):18991–18996.
5. Zhou Y, Morais-Cabral JH, Kaufman A, MacKinnon R (2001) Chemistry of ion coordination and hydration revealed by a K^+ channel-Fab complex at 2.0 A resolution. *Nature* 414(6859):43–48.
6. Cuello LG, Jogini V, Cortes DM, Perozo E (2010) Structural mechanism of C-type inactivation in K(+) channels. *Nature* 466(7303):203–208.
7. Olcese R, Latorre R, Toro L, Bezanilla F, Stefani E (1997) Correlation between charge movement and ionic current during slow inactivation in Shaker K^+ channels. *J Gen Physiol* 110(5):579–589.
8. Saparov SM, Pohl P (2004) Beyond the diffusion limit: Water flow through the empty bacterial potassium channel. *Proc Natl Acad Sci USA* 101(14):4805–4809.
9. Pohl P (2004) Combined transport of water and ions through membrane channels. *Biol Chem* 385(10):921–926.
10. Zeidel ML, Ambudkar SV, Smith BL, Agre P (1992) Reconstitution of functional water channels in liposomes containing purified red cell CHIP28 protein. *Biochemistry* 31(33):7436–7440.
11. Yang B, Verkman AS (1997) Water and glycerol permeabilities of aquaporins 1-5 and MIP determined quantitatively by expression of epitope-tagged constructs in Xenopus oocytes. *J Biol Chem* 272(26):16140–16146.
12. Morais-Cabral JH, Zhou Y, MacKinnon R (2001) Energetic optimization of ion conduction rate by the K^+ selectivity filter. *Nature* 414(6859):37–42.
13. Cordero-Morales JF, et al. (2006) Molecular determinants of gating at the potassium-channel selectivity filter. *Nat Struct Mol Biol* 13(4):311–318.
14. Thompson AN, Posson DJ, Parsa PV, Nimigean CM (2008) Molecular mechanism of pH sensing in KcsA potassium channels. *Proc Natl Acad Sci USA* 105(19):6900–6905.
15. Erokhova L, Horner A, Kügler P, Pohl P (2011) Monitoring single-channel water permeability in polarized cells. *J Biol Chem* 286(46):39926–39932.
16. Levy DI, Deutsch C (1996) Recovery from C-type inactivation is modulated by extracellular potassium. *Biophys J* 70(2):798–805.
17. van Heeswijk MP, van Os CH (1986) Osmotic water permeabilities of brush border and basolateral membrane vesicles from rat renal cortex and small intestine. *J Membr Biol* 92(2):183–193.
18. Finkelstein A (1987) *Water Movement Through Lipid Bilayers, Pores, and Plasma Membranes* (Wiley, New York).
19. Saparov SM, et al. (2006) Mobility of a one-dimensional confined file of water molecules as a function of file length. *Phys Rev Lett* 96(14):148101.
20. Israelachvili JN (1986) Measurement of the viscosity of liquids in very thin films. *J Colloid Interface Sci* 110(1):263–271.
21. Raviv U, Laurat P, Klein J (2001) Fluidity of water confined to subnanometre films. *Nature* 413(6851):51–54.
22. Kestin J, Sokolov M, Wakeham WA (1978) Viscosity of liquid water in the range -8 °C to 150 °C. *J Phys Chem Ref Data* 7(3):941–948.
23. Almers W, Armstrong CM (1980) Survival of K^+ permeability and gating currents in squid axons perfused with K^+-free media. *J Gen Physiol* 75(1):61–78.
24. Cheng WWL, McCoy JG, Thompson AN, Nichols CG, Nimigean CM (2011) Mechanism for selectivity-inactivation coupling in KcsA potassium channels. *Proc Natl Acad Sci USA* 108(13):5272–5277.
25. Saparov SM, Antonenko YN, Koeppe RE, 2nd, Pohl P (2000) Desformylgramicidin: A model channel with an extremely high water permeability. *Biophys J* 79(5):2526–2534.
26. Bhate MP, Wylie BJ, Tian L, McDermott AE (2010) Conformational dynamics in the selectivity filter of KcsA in response to potassium ion concentration. *J Mol Biol* 401(2):155–166.
27. Lockless SW, Zhou M, MacKinnon R (2007) Structural and thermodynamic properties of selective ion binding in a K^+ channel. *PLoS Biol* 5(5):e121.
28. Chakrapani S, Cordero-Morales JF, Perozo E (2007) A quantitative description of KcsA gating II: Single-channel currents. *J Gen Physiol* 130(5):479–496.
29. Finkelstein A, Andersen OS (1981) The gramicidin A channel: A review of its permeability characteristics with special reference to the single-file aspect of transport. *J Membr Biol* 59(3):155–171.
30. Furini S, Beckstein O, Domene C (2009) Permeation of water through the KcsA K^+ channel. *Proteins* 74(2):437–448.
31. Boiteux C, Bernèche S (2011) Absence of ion-binding affinity in the putatively inactivated low-[K^+] structure of the KcsA potassium channel. *Structure* 19(1):70–79.
32. Dani JA, Levitt DG (1981) Binding constants of Li^+, K^+, and Tl^+ in the gramicidin channel determined from water permeability measurements. *Biophys J* 35(2):485–499.
33. Nelson PH (2011) A permeation theory for single-file ion channels: One- and two-step models. *J Chem Phys* 134(16):165102.
34. Piasta KN, Theobald DL, Miller C (2011) Potassium-selective block of barium permeation through single KcsA channels. *J Gen Physiol* 138(4):421–436.
35. Hille B, Schwarz W (1978) Potassium channels as multi-ion single-file pores. *J Gen Physiol* 72(4):409–442.
36. Bernèche S, Roux B (2001) Energetics of ion conduction through the K^+ channel. *Nature* 414(6859):73–77.
37. Thompson AN, et al. (2009) Mechanism of potassium-channel selectivity revealed by $Na(^+)$ and $Li(^+)$ binding sites within the KcsA pore. *Nat Struct Mol Biol* 16(12):1317–1324.
38. Kim I, Allen TW (2011) On the selective ion binding hypothesis for potassium channels. *Proc Natl Acad Sci USA* 108(44):17963–17968.
39. López-Barneo J, Hoshi T, Heinemann SH, Aldrich RW (1993) Effects of external cations and mutations in the pore region on C-type inactivation of Shaker potassium channels. *Receptors Channels* 1(1):61–71.
40. Amiry-Moghaddam M, et al. (2003) Delayed K^+ clearance associated with aquaporin-4 mislocalization: Phenotypic defects in brains of alpha-syntrophin-null mice. *Proc Natl Acad Sci USA* 100(23):13615–13620.
41. Skerra A (1994) Use of the tetracycline promoter for the tightly regulated production of a murine antibody fragment in Escherichia coli. *Gene* 151(1-2):131–135.
42. Heginbotham L, Odessey E, Miller C (1997) Tetrameric stoichiometry of a prokaryotic K^+ channel. *Biochemistry* 36(33):10335–10342.
43. Blunck R, Cordero-Morales JF, Cuello LG, Perozo E, Bezanilla F (2006) Detection of the opening of the bundle crossing in KcsA with fluorescence lifetime spectroscopy reveals the existence of two gates for ion conduction. *J Gen Physiol* 128(5):569–581.
44. Heerklotz H, Tsamaloukas AD, Keller S (2009) Monitoring detergent-mediated solubilization and reconstitution of lipid membranes by isothermal titration calorimetry. *Nat Protoc* 4(5):686–697.
45. Krylova OO, Jahnke N, Keller S (2010) Membrane solubilisation and reconstitution by octylglucoside: Comparison of synthetic lipid and natural lipid extract by isothermal titration calorimetry. *Biophys Chem* 150(1-3):105–111.
46. Knyazev DG, et al. (2013) The bacterial translocon SecYEG opens upon ribosome binding. *J Biol Chem*, 10.1074/jbc.M113.477893.
47. Magde D, Elson EL, Webb WW (1974) Fluorescence correlation spectroscopy. II. An experimental realization. *Biopolymers* 13(1):29–61.
48. Montal M, Mueller P (1972) Formation of bimolecular membranes from lipid monolayers and a study of their electrical properties. *Proc Natl Acad Sci USA* 69(12):3561–3566.